Fair Volatility: A Framework for Reconceptualizing Financial Risk

Sergio Bianchi[a], Daniele Angelini[a]

[a]*Sapienza University of Rome Via del Castro Laurenziano 9 Rome 00161 Italy*

Abstract

Volatility is the canonical measure of financial risk, a role largely inherited from Modern Portfolio Theory. Yet, its universality rests on restrictive efficiency assumptions that render volatility, at best, an incomplete proxy for true risk. This paper identifies three fundamental inconsistencies: (i) volatility is path-independent and blind to temporal dependence and non-stationarity; (ii) its relevance collapses in derivative-intensive strategies, where volatility often represents opportunity rather than risk; and (iii) it lacks an absolute benchmark, providing no guidance on what level of volatility is economically "fair" in efficient markets. To address these limitations, we propose a new paradigm that reconceptualizes risk in terms of predictability rather than variability. Building on a general class of stochastic processes, we derive an analytical link between volatility and the Hurst–Hölder exponent within the Multifractional Process with Random Exponent (MPRE) framework. This relationship yields a formal definition of "fair volatility," namely the volatility implied under market efficiency, where prices follow semi-martingale dynamics. Extensive empirical analysis on global equity indices supports this framework, showing that deviations from fair volatility provide a tractable measure of market inefficiency, distinguishing between momentum-driven and mean-reverting regimes. Our results advance both the theoretical foundations and empirical assessment of financial risk, offering a definition of volatility that is efficiency-consistent and economically interpretable.

Keywords: Volatility, Hurst-Hölder exponent, Multifractional Processes with Random Exponent

Introduction and motivation

Volatility, typically measured as the standard deviation of asset returns, is widely regarded as the preeminent proxy for financial risk in both academic research and investment practice. This convention largely stems from Markowitz's Modern Portfolio Theory, which established variance minimization as the mathematical foundation of portfolio optimization. However, in this work we argue that volatility can represent an incomplete and often misleading measure of true financial risk, and that its justification relies on the belief that markets are ubiquitously efficient, so that properly discounted prices behave like martingales.

Basically, three arguments can be used to support the inconsistency of volatility when more general models than the (sub)martingale one are used to describe price dynamics: (a) volatility's insensitivity to the temporal structure of returns (and more generally to non stationarity, particularly when it affects the dependence of data), (b) its inadequacy in

derivative-heavy strategies, and (c) its inherently relative nature which does not allow to assess whether a given level of volatility is in some sense "*fair*".

a) The Temporal Blindness of Volatility

The most fundamental limitation of volatility as a risk measure lies in its indifference to the order in which returns are generated. Consider the four return series in Figure 1.
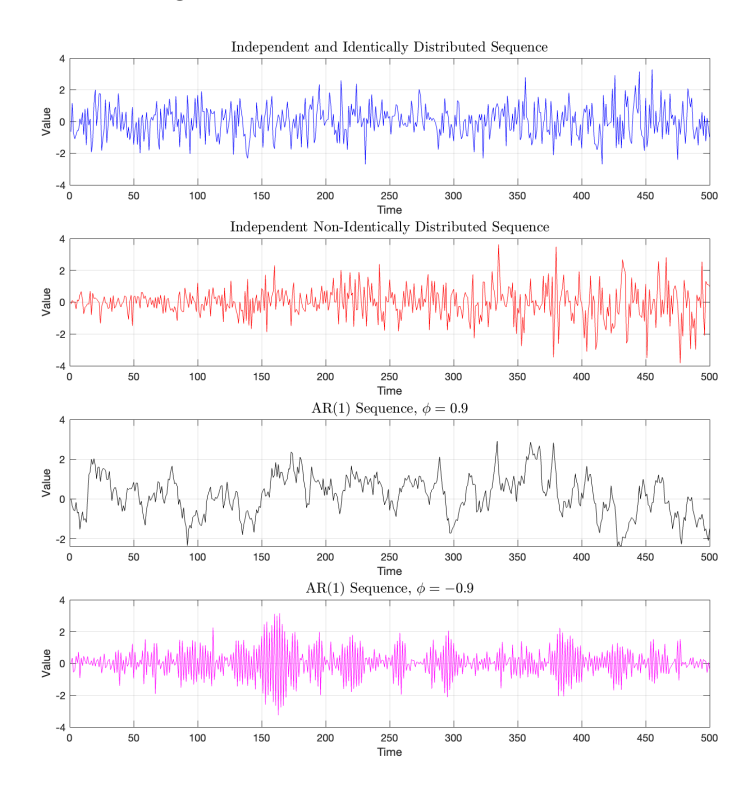

Figure 1: Path-dependent risk characteristics: (Top panel) IID Gaussian noise; (Upper-mid panel) Independent Non Identically distributed Gaussian noise; (Lower-mid panel) AR(1) process ($\phi = 0.9$); (Bottom panel) AR(1) process ($\phi = -0.9$). The four sequences are engineered to have $\sigma = 1$.

They have engineered to display a unit volatility over the entire sample, but despite this, these series present radically different behaviors and risk profiles. The IID process (top panel) represents genuine unpredictability–each price movement provides no information about subsequent movements, as stated by Efficient Market Hypothesis (EMH). The Independent Non-Identically Distributed sequence (upper-middle panel) invalidates the information provided by volatility, unless the process underlying the non-stationarity of the sequence is known. Finally, both the positively and negatively autocorrelated series actually present lower risk: positive autocorrelation (lower-middle panel) generates momentum and persistence, that sophisticated traders might exploit; negative autocorrelation (bottom panel) generates mean-reversion and antipersistence, and a contrarian investor could exploit them because drawdowns tend to reverse more predictably.

Volatility's mathematical formulation discards all temporal information, reducing the complex dynamics of financial time series to a single moment of their distribution. This represents a profound information loss, as the joint distribution of returns contains crucial

risk information that the marginal distribution alone cannot capture. The measure is path-independent in a world where financial risk is inherently path-dependent. It is likewise of limited relevance that most empirical studies conclude that financial returns exhibit no significant autocorrelation beyond very short (minute-level) horizons. Non-stationarity may, in fact, obscure the presence of autocorrelations of opposite sign, where they exist, thereby making the series appear uncorrelated when considered in aggregate. As an illustrative example, consider Figure 2, which shows the effect of concatenating two fractional Gaussian noises (fGns) with different Hurst exponents. While each fGn with a given Hurst parameter is stationary, the resulting concatenated sequence is not. Moreover, the distinctive features of the two processes – the positive long-term autocorrelation of the fGn with $H = 0.75$ and the negative short-term autocorrelation of the fGn with $H = 0.25$ – "disappear" once the two sequences are combined.
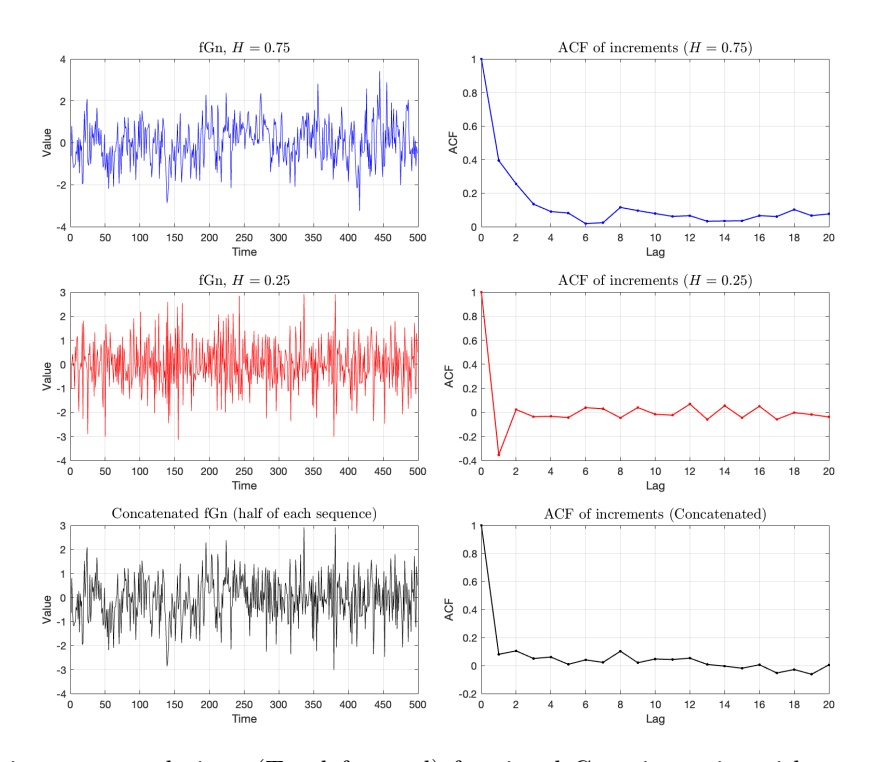

Figure 2: Resetting autocorrelation: (Top left panel) fractional Gaussian noise with parameter $H = 0.75$ (persistent); (Mid left panel) fractional Gaussian noise with parameter $H = 0.25$ (mean-reverting); (Bottom left panel) Queued sequence. The right panels display the three sample autocorrelation functions.

It is perhaps unsurprising that the simple fact that volatility is insensitive to information embedded in the temporal structure of the data has never attracted much attention, either in academia or among practitioners (with the obvious exception of chartists who, in a rather naïve and scientifically fragile manner, attempt to extract signals and rules of thumb for predictability from sequentially generated data). The likely reason lies in the credibility long enjoyed, until quite recently, by the EMH and the apparent plausibility of the argument that, if prices fully and instantaneously incorporate all available information, price changes should be independent. This paradigm dominated both theoretical and practical perspectives for nearly sixty years, leaving little room to distinguish between *return variability* (captured by volatility) and the *return (un)predictability* (which constitutes the true source of financial

risk). When independence of returns, cornerstone of the (sub)martingale model, is assumed the only element that truly matters is the quadratic variation of the process, as it is this quantity that defines and underpins the entire stochastic calculus based on Brownian motion. Hence the central role of volatility (whether historical, realized, or implied), which is nothing more than an estimate of the quadratic variation as the data sampling interval becomes arbitrarily small.

However, when empirical evidence—particularly shocks whose frequency and magnitude are inconsistent with the EMH paradigm—prompted a revision of this overly simplistic view of markets, and stochastic volatility models were introduced to capture patterns such as dependence in squared returns that standard theory could not explain, the issue of reconceptualizing the appropriate way to measure financial risk naturally arises.

b) Derivative Strategies and the Volatility-Risk Disconnect

The relationship between volatility and risk becomes even more tenuous when considering strategies incorporating options or other derivatives. For many such strategies, increased volatility actually enhances expected returns rather than representing risk.

Consider a long straddle position, consisting of both a call and put option at the same strike price. The profitability of this strategy increases with the magnitude of price movements, regardless of direction. The payoff function can be expressed as:

$$\Pi_{\text{straddle}} = \max(S_T - K, 0) + \max(K - S_T, 0) - (C + P) \tag{1}$$

where C and P represent the call and put premiums. The value of this position increases with expected volatility, as captured by the options' implied volatility. Similar dynamics exist for strangles, volatility swaps, and various other derivative structures.

For market makers and volatility traders, volatility represents not risk but opportunity–the raw material from which they extract returns. Their risk exposure relates not to volatility itself but to changes in volatility, volatility-of-volatility, and the complex interplay between different moments of the return distribution.

This demonstrates that the volatility-risk relationship is strategy-dependent rather than universal. What constitutes risk for one market participant may represent opportunity for another, undermining the notion that volatility provides an objective, universal risk metric.

c) The Missing Benchmark: What Volatility Should Efficient Markets Exhibit?

A more profound theoretical problem with volatility as a risk measure lies in the absence of any absolute benchmark. So far, we cannot define what level of volatility corresponds to an "appropriate" (in some sense) degree of risk in an efficient market, because there is no theoretical framework that specifies what the "normal" level of volatility should be. In contrast to asset prices, which have theoretical anchors like discounted cash flow models or arbitrage relationships, volatility lacks any "*fair value*" benchmark. Consequently, while we can compare current volatility to historical levels, this relative approach provides no insight into whether any level is economically justified.

The EMH suggests that prices should fully reflect available information, but offers no prediction about what volatility this process should generate. Should efficient markets exhibit "*low*" volatility as prices smoothly adjust to new information? Or "*high*" volatility

as markets rapidly incorporate complex information? The theory provides no guidance and the absence of a theoretical benchmark makes volatility particularly problematic for regulatory purposes and risk management. Without knowing what level of volatility represents "*normal*" market functioning versus excessive risk-taking, policymakers lack clear criteria for intervention.

The problem is further complicated by the fundamental distinction between realized and implied volatility, and the complex term structure of volatility expectations. The volatility that markets expect (as reflected in option prices) often differs significantly from the volatility that actually materializes, creating additional dimensions of uncertainty.

This paper aims to address the three principal limitations outlined above by proposing a paradigm shift: from assessing mere variability to quantifying predictability, under the general premise that, since markets can experience transient inefficiencies, the degree of predictability may vary over time (this is what can actually generate autocorrelation in the squared returns in a very general modelling setting). When the market is efficient (*sideways market*), unpredictability – not volatility! – is at its highest; conversely, when the market is inefficient, some degree of predictability can be observed. The effects on volatility depend on the type of inefficiency. If inefficiency generates positive autocorrelation in returns (*momentum market*), this will result in lower variability/volatility than that observed in the efficient case; conversely, if inefficiency triggers negative autocorrelation in returns (*reversals market*), this will generate higher variability/volatility than in the efficient case.

We will establish two key results.

First, we propose a very general class of stochastic processes capable of capturing the intrinsic link between market predictability and observed volatility. Within this framework, volatility can be expressed as a direct function of the underlying predictability of the price series. This theoretical relationship enables the formal derivation of a "fair volatility" benchmark—defined as the volatility level expected under market efficiency, where prices exhibit semi-martingale behavior.

Second, we provide extensive empirical evidence from global equity indices that strongly corroborates the proposed model. This analysis not only validates the theoretical construct but also provides a quantifiable metric for assessing deviations from market efficiency, distinguishing between periods of momentum and mean-reversion.

The structure of this paper is organized in the following manner. Section 1 revisits the theoretical foundations to formally derive the analytical relationship linking the pointwise standard deviation to the Hurst exponent within the Multifractional Process with Random Exponent (MPRE) framework. Subsequently, Section 2 provides a financial justification for the Hurst-Hölder regularity's role as a superior risk metric and elucidates its capacity to integrate principles from both rational and behavioral finance. Section 3 offers a concise overview of the fundamental properties characterizing established estimators for the Hurst–Hölder exponent. This is followed by Section 4, which details an empirical analysis furnishing robust evidence in support of the theoretically proposed relationship. The paper concludes with Section 5, which synthesizes the key findings and presents final remarks.

1. Framework

1.1. Theoretical Foundations

Under the Efficient Market Hypothesis (EMH) [26], asset prices fully incorporate all available information. Given a filtered probability space $(\Omega, \mathcal{F}, (\mathcal{F}_t)_{t\in\mathbb{R}}, \mathbb{P})$, this principle requires the discounted price process $\hat{S}(t)$ to be a martingale, either under the physical measure $\mathbb{P}$ or, more commonly, under a risk-neutral measure $\mathbb{Q}$, i.e.

$$\mathbb{E}^{\mathbb{Q}}(\hat{S}(t)|\mathcal{F}_\tau) = \hat{S}(\tau), \qquad (\tau \leq t).$$

The martingale property can be investigated through variation processes. Specifically: (a) the total variation of $\hat{S}(t)$ over any interval $[0, t]$ is infinite (except for degenerate cases); (b) its quadratic variation $[\hat{S}]_t$ is finite and uniquely identifies the martingale component; (c) higher-order variations (for $p > 2$) vanish for martingales but not for more complex processes (e.g. Hermite processes). Hence, while total variation is too crude and higher-order variations degenerate, quadratic variation is the central tool for classifying martingales. This result underlies Itô calculus and no-arbitrage pricing. Denoted by $\{W(t)\}_{t\in\mathbb{R}}$ the standard Brownian motion and by $X(t) = \sigma W(t)$ for a constant $\sigma > 0$, the quadratic variation satisfies [37] $[X](t) = \sigma^2 t$, so that realized volatility is recovered as $\sigma = \sqrt{\frac{[X](t)}{t}}$. Thus, the irregularity of Brownian motion is entirely encoded in its quadratic variation, establishing volatility as the natural measure of financial risk. This justifies, within the EMH framework, the focus on volatility as the sole risk metric.

Nevertheless, empirical evidence demonstrates that volatility is time-varying, rendering constant-volatility Brownian models unrealistic. This has led to the development of stochastic volatility models of the form

$$dS(t) = \mu\, S(t)\, dt + \sigma(t)\, S(t)\, dW(t),$$

or even more general Itô diffusions with stochastic diffusion coefficients. In these models, the discounted price $\hat{S}(t)$ remains a martingale provided that: (a) the drift is zero (or adjusted under the risk-neutral measure), and (b) the volatility process is adapted and arbitrage-free. The expectation under $\mathbb{Q}$ of its quadratic variation is

$$\mathbb{E}^{\mathbb{Q}}\left([\hat{S}](t)\right) = \mathbb{E}^{\mathbb{Q}}\left(\int_0^t \sigma^2(\tau)\hat{S}^2(\tau)\, d\tau\right).$$

In mean-reverting models, quadratic variation stabilizes in the long run but remains path-dependent. Since realized variance estimates quadratic variation, its discrepancy from expected quadratic variation forms the basis of volatility trading (e.g. variance swaps, VIX derivatives). More generally, whether in constant or stochastic volatility settings, the randomness of returns is fully determined by the growth of quadratic variation—linear in t for Brownian motion, or integrated variance otherwise.

A natural extension involves volatility processes with memory, better capturing market behavior. A general form is

$$\begin{cases} dS(t) = \mu\, S(t)\, dt + \sigma(t)\, S(t)\, dW(t), \\ d\sigma(t) = \alpha(\sigma(t), t)\, dt + \nu(\sigma(t), t)\, dW^H(t), \end{cases} \tag{2}$$

where $\sigma(t)$ is driven by a fractional Brownian motion (fBm) $W^H(t)$ with Hurst exponent H. For $H > 1/2$, the volatility displays long memory and smoothness [21], while for $H < 1/2$, it is rough and short-memory [29]. For instance, if $\alpha(\sigma(t), t) = -\lambda\sigma(t)$ and $\nu(\sigma(t), t) = \nu$, $\sigma(t)$ follows a fractional Ornstein–Uhlenbeck process.

A different approach that produces patterns similar to those obtained by (2) uses the *Multifractional Processes with Random Exponents* (MPRE) [6, 3, 36], which generalizes fBm by allowing time-varying memory or roughness. Before introducing MPRE, the key properties of fBm will be recalled in order to clarify the generalization.

1.2. Fractional Brownian Motion (fBm)

Fractional Brownian Motion (fBm) [33, 38], denoted $W^H(t)$, is a continuous-time Gaussian process starting at zero with stationary increments, parameterized by a Hurst exponent $H \in (0, 1)$. Its integral representation is

$$W^H(t) = \frac{1}{\Gamma\left(H + \frac{1}{2}\right)} \int_{-\infty}^{t} \left[(t - s)_+^{H-1/2} - (-s)_+^{H-1/2} \right] dW(s), \tag{3}$$

where $(\cdot) = \max(0, \cdot)$, with variance of increments given by

$$\mathbb{E}\left[(W^H(t + T) - W^H(t))^2 \right] = V_H T^{2H}.$$

Here V_H is the variance of unit-lag increments, explicitly [44, 23]

$$
\begin{aligned}
V_H &= \frac{1}{\Gamma\left(H + \frac{1}{2}\right)^2} \left\{ \frac{1}{2H} + \int_1^{\infty} \left[u^{H-1/2} - (u - 1)^{H-1/2} \right]^2 du \right\}, \\
&= \frac{\Gamma(1 - 2H)}{\pi H} \cos(\pi H) \\
&= \frac{\Gamma(H)\Gamma(1 - H)}{\pi \Gamma(1 + 2H)} \\
&= \frac{\Gamma(2 - 2H) \cos(\pi H)}{\pi H (1 - 2H)} \\
&= \frac{1}{2H \sin(\pi H)\Gamma(2H)} =: \frac{A(H)}{\Gamma(H + 1/2)^2}.
\end{aligned}
$$

The above equalities summarize the different expressions that can be found in literature for V_H and are explictly proved in [10]. In particular, in the last equality, $A(H)$ is the quantity considered for the covariance function by [36] (cfr. equation (28)). This relation will be useful in section 1.3 to characterize the local behavior of a specific MPRE.

The covariance function of fBm is:

$$\mathbb{E}[W^H(t)W^H(s)] = \frac{V_H}{2} \left(|t|^{2H} + |s|^{2H} - |t - s|^{2H} \right), \quad t, s \geq 0 \tag{4}$$

while the covariance function of its increments $W^H(t + h) - W^H(t)$ reads as

$$\gamma_H(k; h) = \frac{V_H}{2} \left(|k + h|^{2H} - 2|k|^{2H} + |k - h|^{2H} \right) \tag{5}$$

The crucial parameter is the Hurst exponent, which governs the process's properties and roughness:

- $H = 1/2$: Brownian motion (independent increments).

- $H > 1/2$: Persistent, long-memory process. Increments are positively correlated.

- $H < 1/2$: Anti-persistent, short-memory process. Increments are negatively correlated.

1.3. Multifractional Process with Random Exponent

As established in the preceding section, the assumption of a constant Hurst exponent (which means a constant volatility) is often empirically untenable, particularly for processes characterized by structural breaks, regime shifts, or heteroskedastic dynamics—hallmark features of stochastic volatility models. To overcome this limitation inherent in fBm, the framework has been extended through several generalizations[1]. Among these, one of the most flexible and encompassing frameworks is provided by the *Multifractional Process with Random Exponent* (MPRE). The seminal work of [6, 4] constructed an initial MPRE variant via random wavelet series, demonstrating that—under mild conditions—the local roughness (or Hölder regularity) of the sample paths at a point t is directly governed by the value of the functional parameter $H(t)$, thus justifying its designation as the Hurst-Hölder exponent.

A significant constraint of this original MPRE construction, however, is its incompatibility with the standard Itô calculus framework. To remedy this theoretical drawback, a subsequent and operationally distinct MPRE formulation was introduced by [3] and further generalized in [36]. It is this latter class of processes that will serve as the foundational model for the subsequent analysis. In particular, although the framework is very general, given the filtered probability space $(\Omega, \mathcal{F}, (\mathcal{F}_s)_{s \in \mathbb{R}}, \mathbb{P})$, we will refer to the following specification of MPRE, which generalizes equation (3):

$$X(t) = \int_{-\infty}^{t} \nu(s) \left[(t-s)_+^{H(s)-1/2} - (-s)_+^{H(s)-1/2} \right] dW(s), \qquad (6)$$

where $\nu(s) > 0$ plays a role similar to that of the normalization factor V_H for $W^H(t)$ and $H(s) \in (0,1)$ is a random variable or even an $\mathcal{F}_s$-adapted stochastic process.

Remark 1. *In the particular case where all the random variables $H(s)$ are equal to the same deterministic constant H, $X(t)$ reduces to the $W^H(t)$*

Remark 2. *Assuming that $H(t)$ and $\nu(t)$ are stationary and $\mathcal{F}_s$-adapted, [36] prove that*

$$\mathbb{E}(X(t)X(s)) = \mathbb{E}\left[\nu(0)^2 \frac{A(H(0))}{2} \left(|t|^{2H(0)} + |s|^{2H(0)} - |t-s|^{2H(0)} \right) \right] \qquad (7)$$

provided that the latter value is finite for all $t, s \in \mathbb{R}$.

---

[1]Notable extensions include the multifractional Brownian motion (mBm) [41, 8] and its generalized variant (GmBm) [5], bifractional Brownian motion [30], mixed fBm [18], fractional Riesz-Bessel motion [2], the Multi-fractional Generalized Cauchy Process [34], and Multifractional Processes with Random Exponents (MPRE) [6] (see [35] for a comprehensive review). For other interesting directions, see also [25, 24].

The MPRE offers a highly general and parsimonious framework for modeling price dynamics. Its key strength lies in its flexibility to capture both efficient market phases, characterized by a Hurst exponent $H(t) = 1/2$, and disequilibrium phases exhibiting momentum ($H(t) > 1/2$) or mean-reversion ($H(t) < 1/2$). Under the assumption that asset prices follow an MPRE, a critical question arises: what is the relationship between the pointwise variance (or standard deviation) of the process and the Hurst function $H(t)$? Establishing this link is fundamental for our purpose, since it would ensure that the resulting volatility measure, $\sigma(t)$, remains path-sensitive. Consequently, a H-based volatility measure $\sigma(t)$ would not discard crucial information but instead encapsulate the process's time-varying memory properties, providing a more informative measure of latent risk.

To address the above question, we prove the following, which generalizes equation (15) in [10] for an lag $h \neq 1$.

Proposition 1 (Standard deviation of MPRE increments). *The MPRE*

$$X(t) = \int_{-\infty}^{t} \nu(s) \left[(t-s)_+^{H(s)-\frac{1}{2}} - (-s)_+^{H(s)-\frac{1}{2}} \right] dW(s),$$

with a random Hurst function $H(s) \in (0,1)$ and a volatility factor $\nu(s) > 0$ has (conditional) standard deviation of a short–lag increment given by

$$\mathrm{sd}\left(X(t+h) - X(t) \,\middle|\, \mathcal{F}_t^{H,\nu} \right) \sim |h|^{H(t)} \, \nu(t) \, \sqrt{A(H(t))}, \qquad h \to 0, \tag{8}$$

where

$$A(H) = \frac{\Gamma\left(H + \frac{1}{2}\right)^2}{2H \, \sin(\pi H) \, \Gamma(2H)}.$$

Here $\mathcal{F}_t^{H,\nu} := \sigma\big(\{(H(s), \nu(s)) : s \leq t\}\big)$ is the σ–field generated by (H, ν) up to time t.

Proof. See Annex 1.

Remarks.

- The proof crucially used **H1** to apply the conditional Itô isometry with respect to $\mathcal{F}_t^{H,\nu}$. The continuity assumption **H2** yields the "local freezing" $\nu_{t \pm o(1)} \to \nu_t$ and $H_{t \pm o(1)} \to H_t$, which justifies dominated convergence in Step 4.

- The constant $A(H)$ coincides with the variance of the unit increment of the (non–normalised) fractional Brownian motion associated with the Mandelbrot–Van Ness kernel used here; equivalently, if one rescales the kernel by the factor $c_H := \Gamma\left(H + \frac{1}{2}\right)^{-1} \sqrt{2H \sin(\pi H) \Gamma(2H)}$, then $\mathrm{Var}(W^H(t+h) - W^H(t)) = |h|^{2H}$.

- Standard deviation (8) is consistent with the autocovariance function (7), from which it directly follows the autocovariance function $\gamma(h)$ of the increment process $X(t+1) - X(t)$

$$\gamma(h) = \mathbb{E}\left[\nu(0)^2 \frac{A(H(0))}{2} \left(|h+1|^{2H(0)} - 2|h|^{2H(0)} + |h-1|^{2H(0)} \right) \right]$$

9

2. Path Hurst-Hölder Regularity as a Risk Indicator and a Bridge Between Rational and Behavioral Finance

The Hurst exponent $H(t)$ provides a theoretically rigorous measure of pathwise regularity, quantifying deviations from the semimartingale framework. Its critical value, $H(t) = 1/2$, corresponds to efficient martingale dynamics, making it a natural foundation for modeling volatility in non-semimartingale settings—particularly those exhibiting roughness. This approach offers distinct advantages over conventional volatility measures:

a) Sensitivity to Autocorrelation Structure:. Unlike volatility, which is a scale-dependent measure of dispersion, the Hurst-Hölder exponent is scale-invariant and directly responsive to the autocorrelation structure of returns. Processes with differing temporal dependencies can exhibit identical volatility yet possess distinct $H(t)$ values, as autocorrelation intrinsically governs the smoothness—and hence the regularity—of sample paths. The link between volatility and $H(t)$ ensures that no loss of information occurs when using $H(t)$ or when referring volatility $\sigma(t)$ to the corresponding value $H(t)$ via equation (8).

b) An Absolute Benchmark for Market Efficiency:. Volatility is a relative measure, only indicating whether current variability is high or low relative to the past. It offers no concept of "fair" volatility consistent with market efficiency. In contrast, $H(t)$ has a natural absolute benchmark: $H(t) = 1/2$ corresponds precisely to the efficient dynamics of a Brownian martingale. The deviation $|H(t) - 1/2| \in (0, 1/2)$ thus provides a direct, quantitative measure of market inefficiency and predictability [14].

c) Predictive Content via Mean-Reversion:. Empirically, the time-varying Hurst exponent displays stationarity, mean-reversion, and a normal distribution centered at $1/2$—properties consistent with a fractional Ornstein-Uhlenbeck specification for $H(t)$ [17, 11, 42, 28, 39]. The fact that financial markets exhibit a tendency to revert toward the efficient state $H(t) = 1/2$, suggests to use the magnitude of deviation $|H(t) - 1/2|$ as a indicator for the timing of mean-reversion. This offers a stochastic formalization of the adage "what goes up must come down" and a parsimonious theoretical explanation for empirical phenomena like the reversal effects documented by [22].

Table 1: Financial interpretation of $H(t)$

$H(t)$	Stochastic properties	Behavioral interpretation	Market implications
$> \frac{1}{2}$	Persistence, smooth paths, $[X](t) = 0$	New information confirms existing positions	*Unfair low* volatility, momentum, positive inefficiency, overconfidence, underreaction
$= \frac{1}{2}$	Independence, martingale behavior, $[X](t) = t$ (Brownian)	Information fully incorporated into prices	*Fair* volatility, sideways market, informational efficiency
$< \frac{1}{2}$	Mean-reversion, rough paths, $[X](t) = \infty$	New information disrupts existing positions	*Unfair high* volatility, reversals, negative inefficiency, overreaction

As summarized in Table 1 [15, 10], the Hurst-Hölder exponent provides a holistic characterization of market states by discerning both the *magnitude* and *structure* of variability. It classifies local dynamics into:

- **Momentum markets** ($H(t) > 1/2$): trends and speculative bubbles.
- **Efficient markets** ($H(t) \approx 1/2$): sideways movement with minimal predictability.
- **Reversal markets** ($H(t) < 1/2$): overreaction and rapid price adjustments.

Thus, $H(t)$ moves beyond volatility by jointly addressing the "*how much*" and "*how*" of price variation, offering a unified metric for efficiency, predictability, and regime classification. Moreover, Table 1 summarizes that $H(t)$ provides a mathematical basis for integrating Rational and Behavioral Finance within a bounded rationality framework. Rather than being conflicting paradigms, they represent alternating market states, with $H(t)$ explicitly quantifying the transition between them. A shift away from the efficient benchmark ($H(t) = 1/2$) signals the emergence of systematic irrationality, which the model characterizes as either trend-persistence (bubbles, overconfidence) or anti-persistence (reversals, overreaction).

3. Estimation of the Hurst-Hölder parameter

In the previous section, an analytical relationship was established between the Hurst exponent and the standard deviation, both referred to the generic time t. Therefore, it is clear that the question becomes how to estimate $H(t)$, but detailing the methodologies available for this purpose is beyond the scope of this article. Here we will simply note that the problem of dynamically estimating the time-dependent Hurst–Hölder exponent has been extensively addressed in the statistical and econometric literature. Numerous methodologies have been proposed for this purpose, including variation-statistical approaches, wavelet-based techniques, and local likelihood methods [31, 32, 7, 19, 20, 40, 45].

For the empirical application in this study, we adopt a well-established estimation procedure detailed in [12, 1, 27]. This method leverages the local asymptotic self-similarity of multifractional processes, which ensures that within a sufficiently small neighborhood of any time t the process behave like an fBm. Therefore, in a small window of size δ centered around t the increments are approximately normally distributed with mean zero and variance proportional to $H(t)$. The core of the approach involves constructing a moment-based estimator, $\hat{H}_t^{2,\delta,n}$, which exhibits favorable statistical properties. As demonstrated by [9, 43] and formalized in [1], this estimator can be refined to achieve unbiasedness and a convergence rate of $\mathscr{O}(\delta^{-1/2}(\log n)^{-1})$.

A key implication of this framework is the establishment of a direct functional relationship between the estimated Hurst exponent and local volatility.

Under the null hypothesis of market efficiency ($H(t) = 1/2$), the sampling distribution of the estimator is known [13], enabling the construction of confidence intervals for statistical inference since

$$\hat{H}_t^{2,\delta,n}|_{H(t)=1/2} \sim \mathscr{N}\left(\frac{1}{2}, \frac{1}{2\delta \ln^2(n-1)}\right). \tag{9}$$

In the subsequent empirical analysis, all estimates are computed using a rolling window of $\delta = 20$ trading days.

4. Empirical analysis

In this section, we will apply the methodology presented in the preceding sections to the set of 14 daily global stock indices summarized in Table 2.

Table 2: Dataset

Index	Country	Ticker	Start Date	End Date	Size
S&P 500 Index	USD	SPX	1927-12-30	2025-08-22	24,527
NASDAQ Composite Index	USD	CCMP	1971-02-05	2025-08-22	13,753
EURO STOXX 50® Price EUR	EUR	SX5E	2007-03-30	2025-08-22	4,612
FTSE 100 Index	UK	UKX	1984-01-03	2025-08-22	10,519
Hang Seng Index	Hong Kong	HSI	1986-12-31	2025-08-22	9,538
FTSE Bursa Malaysia KLCI Index	Malaysia	KLCI	1993-12-03	2025-08-22	7,795
KOSPI Index	Korea	KOSPI	1996-12-11	2025-08-22	7,067
MOEX Russia Index	Russia	IMOEX	2013-03-05	2024-06-14	2,795
NIFTY 50 Index	India	NIFTY	2007-09-17	2025-08-22	4,399
Nikkei 225	Japan	NKY	1965-01-05	2025-08-22	14,909
SET Index (Thailand)	Thailand	SET	1996-12-11	2025-08-22	7,000
Shanghai Composite Index	Shanghai	SHCOMP	1997-07-02	2025-08-22	6,819
FTSE Straits Times Index	Singapore	FSSTI	1987-12-28	2025-08-22	9,408
Taiwan Stock Exchange Weighted Index	Taiwan	TWSE	1997-07-02	2025-08-22	6,900

We assume that the pricing process can be represented as an MPRE—a parsimonious hypothesis which, as previously discussed, is capable of encompassing and summarizing a wide range of models commonly employed to describe financial dynamics. Under this assumption, we estimate the parameter $H(t)$ and the function $\nu(t)$ of the process. Subsequently, using the expression derived in Proposition 1, we obtain an estimate of volatility, which we compare with historical volatility independently computed through the traditional rolling-window standard deviation formula. The comparison between these two estimates enables us to pursue two main objectives.

Validation of the model: the proximity between the two volatility measures provides evidence of the goodness of the MPRE as a model for capturing the dynamics of stock indices.

Interpretation of volatility within a benchmark framework: volatility can be expressed relative to the benchmark that corresponds to the value expected under market efficiency, i.e., when the price process follows a semimartingale. Concretely, the confidence interval associated with $H(t) = 1/2$ (see equation (9)), when transformed through relation (8), yields the bounds of the confidence interval for volatility. This allows us to interpret volatility values within the interval as *fair*, while those outside it may be regarded as *unfairly low* or *unfairly high*, in line with the descriptions provided in Table 1.

Figures from 3 to 16 display, for each index, the estimate of the parameter $H(t)$ along with the confidence interval around the value $1/2$ that characterizes market efficiency, highlighted as the green area (top panel); the theoretical volatility calculated using equation (8) (in red) and the empirical historical volatility (in blue) estimated using the classic standard deviation formula calculated on a rolling-window of $\delta = 20$ days (again, the green region indicates the 95% confidence interval for fair volatility) (middle panel); the function $\nu(t)$ estimated using equation (8) (bottom panel).

Table 3: Summary statistics of estimates.

Index	SPX	CCMP	SX5E	UKX	HSI	KLCI	KOSPI
Hurst-Hölder parameter							
Mean	0.5090	0.5320	0.4463	0.4986	0.5307	0.5527	0.4910
St.Dev	0.0520	0.0563	0.0542	0.0460	0.0486	0.0651	0.0608
Range	0.3507	0.3528	0.3297	0.3197	0.3490	0.4451	0.3372
Kurtosis	3.7684	3.1854	3.4357	4.1583	4.4781	4.0574	2.6381
Skewness	-0.6910	-0.5506	-0.5136	-0.8272	-0.8968	-0.7992	-0.4435
95% Confidence interval	[0.469,0.531]	[0.467,0.533]	[0.463,0.537]	[0.467,0.533]	[0.466,0.534]	[0.465,0.535]	[0.465,0.535]
ADF test							
pValue	0.001	0.001	0.001	0.001	0.001	0.001	0.001
Stat	-10.459	-7.908	-5.823	-7.783	-7.712	-6.201	-6.166
cValue	-3.412	-3.412	-3.414	-3.412	-3.412	-3.413	-3.413
Historical volatility							
Mean	0.0102	0.0108	0.0128	0.0097	0.0143	0.0094	0.0145
St.Dev	0.0084	0.0084	0.0089	0.0066	0.0108	0.0106	0.0106
Range	0.0900	0.0734	0.0687	0.0680	0.1371	0.1505	0.0712
Kurtosis	22.7043	15.5307	15.0786	26.9594	46.9586	74.2495	8.1972
Skewness	3.6800	2.9840	2.9203	3.9678	5.2672	6.8706	2.0563
95% C.I. fair volatility	[0.005,0.009]	[0.006,0.012]	[0.010,0.021]	[0.007,0.014]	[0.007,0.014]	[0.008,0.016]	[0.008,0.017]

Index	IMOEX	NIFTY	NKI	SET	SHCOMP	FSSTI	TWSE
Hurst-Hölder parameter							
Mean	0.4983	0.4986	0.5030	0.5283	0.5385	0.5181	0.4967
St.Dev	0.0589	0.0566	0.0516	0.0613	0.0539	0.0528	0.0524
Range	0.4427	0.3452	0.3769	0.3712	0.3136	0.3282	0.2942
Kurtosis	7.3283	4.0497	3.1408	2.9693	2.7638	3.3122	2.4874
Skewness	-1.3776	-0.9113	-0.1315	-0.2554	-0.2764	-0.6884	-0.2981
95% Confidence interval	[0.461,0.539]	[0.463,0.537]	[0.468,0.532]	[0.465,0.535]	[0.465,0.535]	[0.466,0.534]	[0.465,0.535]
ADF test							
pValue	0.004	0.001	0.001	0.001	0.001	0.001	0.001
Stat	-4.274	-5.227	-9.735	-6.562	-6.748	-7.591	-6.790
cValue	-3.414	-3.414	-3.412	-3.413	-3.413	-3.412	-3.413
Historical volatility							
Mean	0.0124	0.0116	0.0115	0.0126	0.0134	0.0101	0.0124
St.Dev	0.0165	0.0092	0.0075	0.0090	0.0079	0.0071	0.0072
Range	0.1875	0.0757	0.0986	0.0669	0.0488	0.0698	0.0452
Kurtosis	90.1554	19.8448	23.4569	10.4266	5.5878	15.7488	5.8632
Skewness	8.6810	3.5896	3.2003	2.3386	1.6055	2.9147	1.5726
95% C.I. fair volatility	[0.013,0.027]	[0.011,0.021]	[0.006,0.012]	[0.008,0.017]	[0.009,0.017]	[0.007,0.015]	[0.009,0.017]

Figure 3: SPX Index
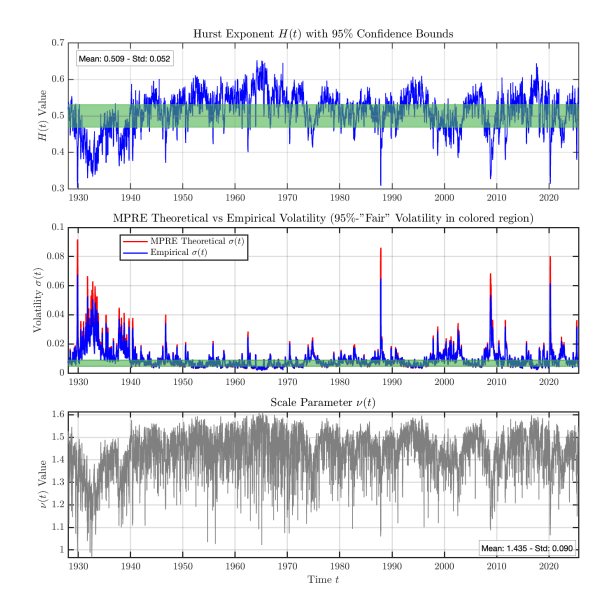

Figure 4: CCMP Index
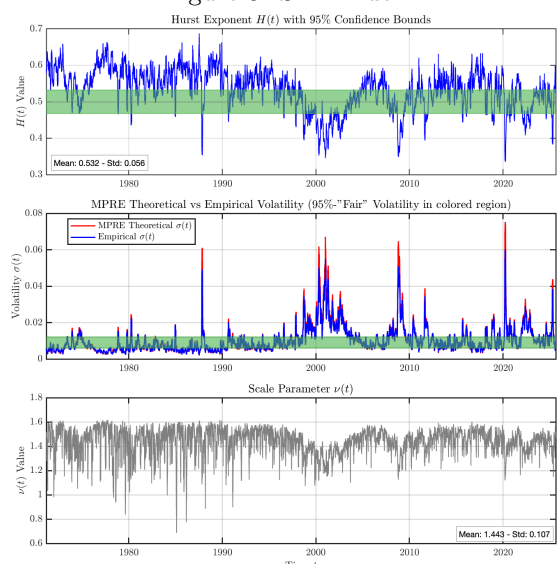
Figure 5: SX5E

Figure 6: UKX Index
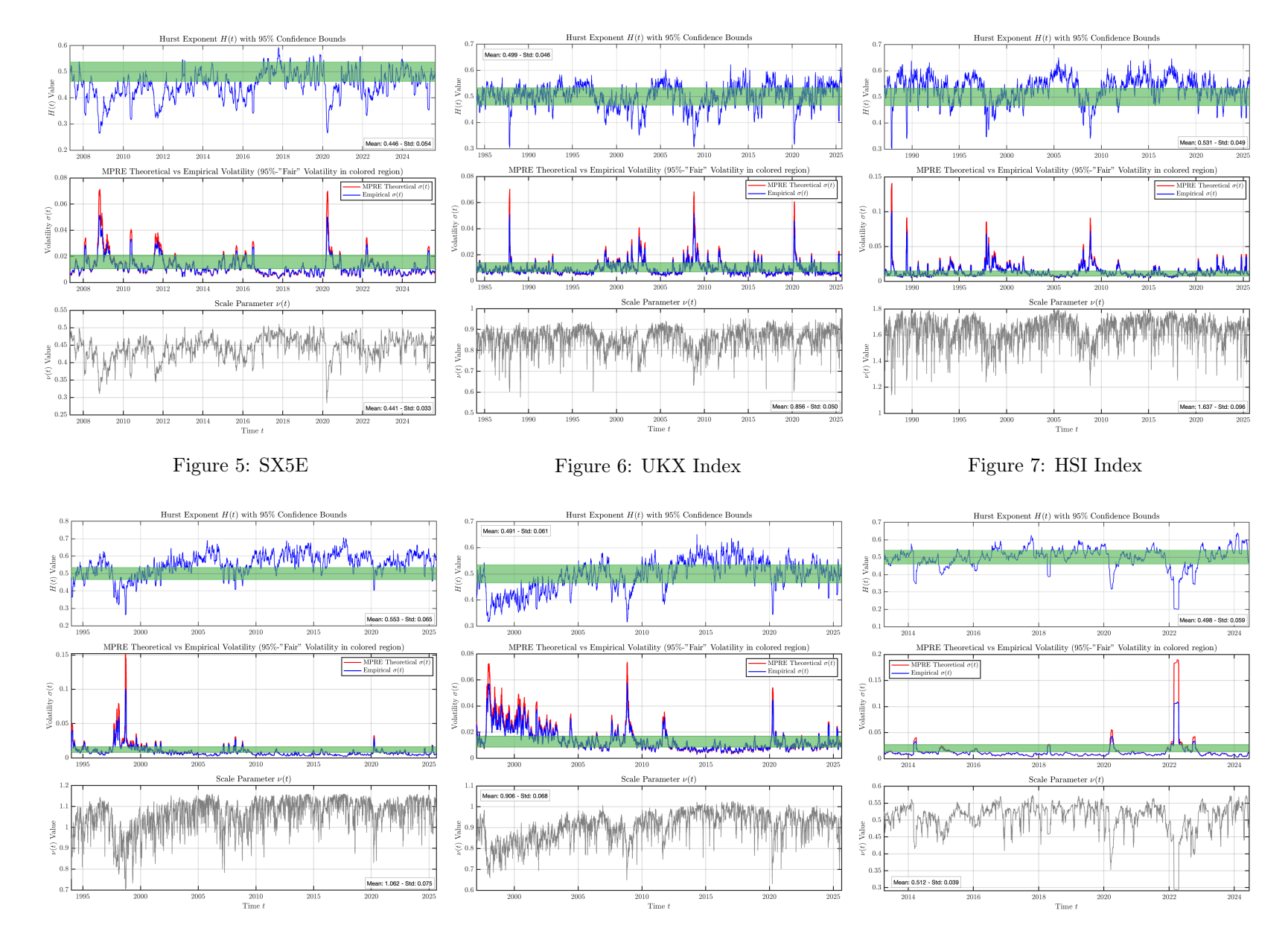

Figure 7: HSI Index

Figure 8: KLCI Index

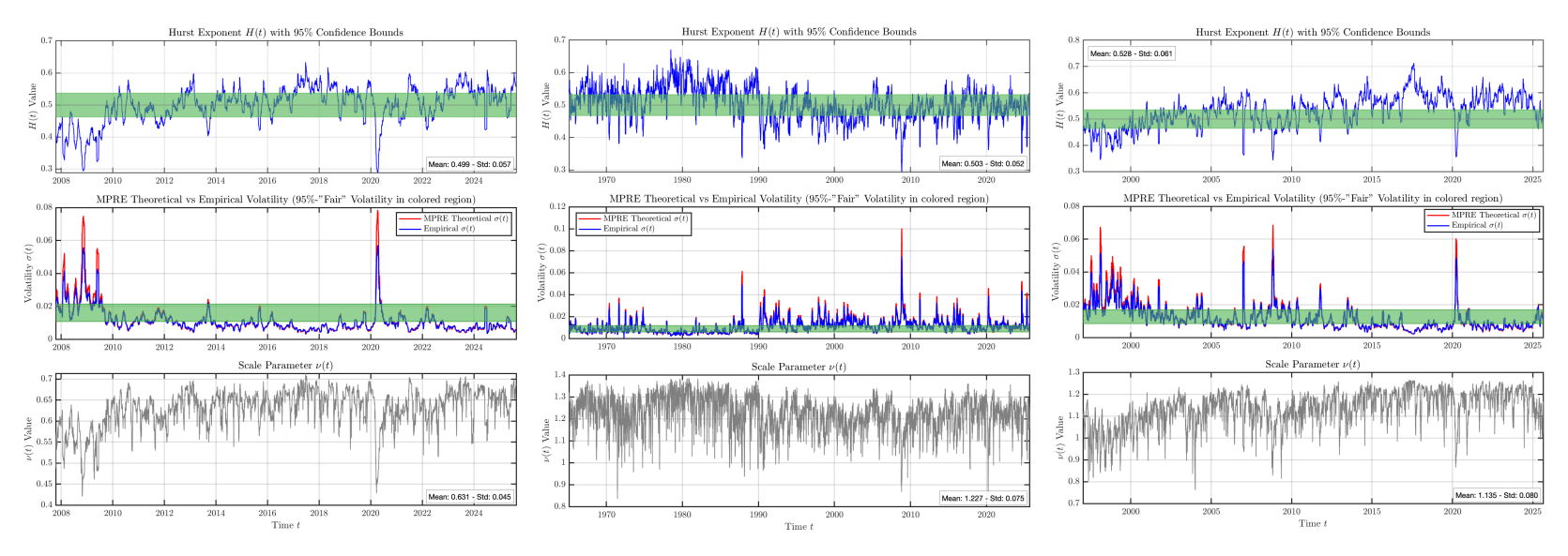Figure 9: KOSPI Index

Figure 10: IMOEX Index

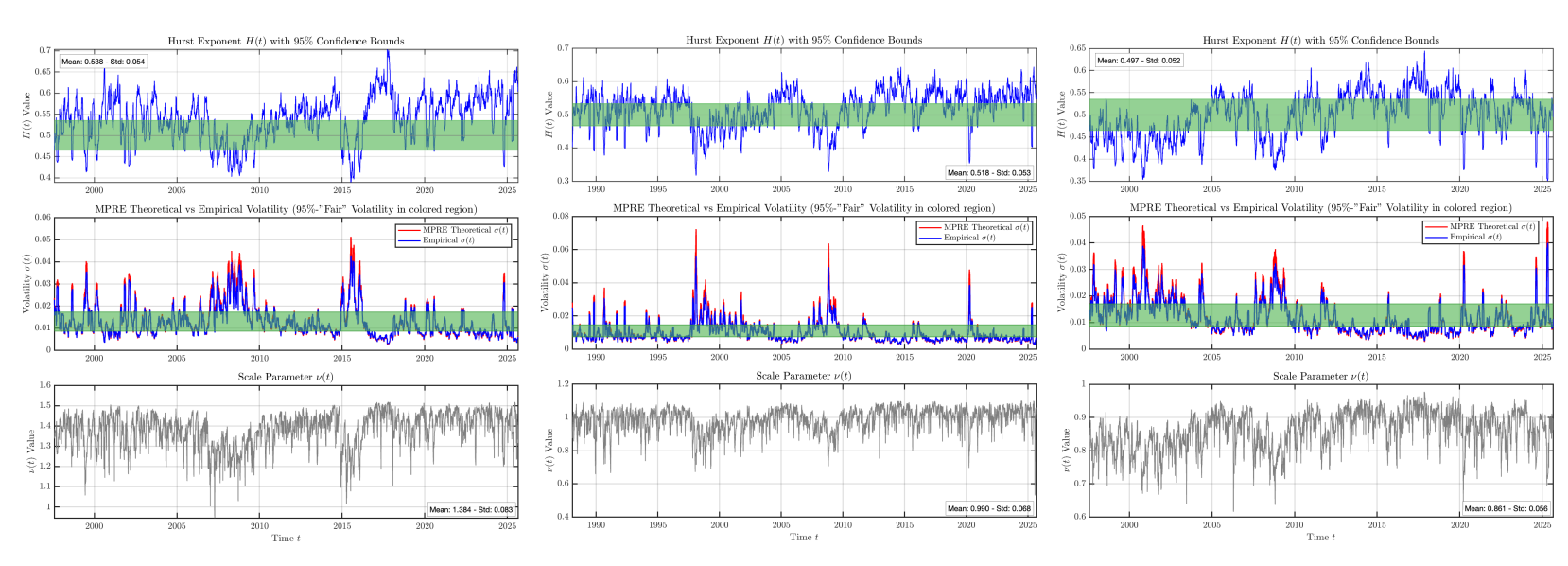Figure 11: NIFTY Index

Figure 12: NKI Index

Figure 13: SET Index

Figure 14: SHCOMP Index

Figure 15: FSSTI Index

Figure 16: TWSE Index

16

4.1. Discussion of results

The broad spectrum of samples considered in the empirical analysis demonstrates the existence of well-defined patterns in the time evolution of the estimated Hurst-Hölder parameter:

1. the sequences exhibit remarkable stability, irrespective of the specific market, the historical horizon under review, or the length of the time series employed. The Augmented Dickey Fuller (ADF) test for trend stationarity reveals that in all cases the estimated sequences are stationary.

2. All series display a tendency to revert toward the efficiency-submartingale-no arbitrage benchmark value of $H(t) = 1/2$. Moreover, for 11 out of the 14 indexes, the averaged $\hat{H}_t^{2,\delta,n}$ lies within the 95% confidence interval. The only exceptions to this regularity are SX5E (0.4463), KLCI (0.5527), and SHCOMP (0.5385), although in this case the result is borderline with respect to the upper threshold equal to 0.535.

3. The roughness of the estimated sequences, together with their pronounced tendency to cluster around $H(t) = 1/2$, is highly meaningful from a financial standpoint. It suggests that when markets deviate from informational efficiency, they exhibit a propensity to revert toward it, thereby restoring equilibrium. This appears to be the consequence of a continuous interplay of opposing disequilibria.

4. The values of kurtosis of $\hat{H}_t^{2,\delta,n}$ (between 2.64 and 4.48, with the exception of IMOEX with 7.33) and the small skewness (between -0.91 and -0.13, with the exception of IMOEX with -1.38) indicate that at first glance a good model for the distributions of the estimated $H(t)$ could be the normal distribution.

5. The slight left skewness of the distribution of $\hat{H}_t^{2,\delta,n}$ indicates the frequency of large negative variations in the parameter relative to positive variations. The former typically occur during market crashes and align with the asymmetric impact that new information has on market participants. In fact, it is improbable that new information can abruptly bolster market confidence in a trend, whereas it is more likely to destabilize the market. Confidence reinforcement is inherently a gradual process (reflected in small positive changes in $H(t)$), whereas confidence erosion often constitutes an instantaneous shock when new information contradicts past beliefs or heightens uncertainty about the future.

6. The deviations of the Hurst–Hölder exponent from $1/2$ are both too frequent and too persistent for one to maintain the simplistic claim that arbitrage opportunities are always and immediately eliminated by self-correcting market mechanisms. Rather, what emerges is a systematic alternation across all indices between phases characterized by efficiency and phases of inefficiency of either a *positive* type ($H(t) > 1/2$, momentum behavior) or a *negative* type ($H(t) < 1/2$, reversal behavior). This alternation is not incidental but instead represents a robust and recurrent empirical regularity, as can be seen in the frequency and magnitude of the deviations of $H(t)$ from $1/2$ in Figures 3–16.

The patterns summarized above are conistent with and actually support the efforts to model stochastic volatility (as well as the $H(t)$ process in MPRE) as a fractional Ornstein-Uhlenbeck processes [29, 1, 16].

Within this interpretative framework and with reference to the stock price $S(t)$, the

notion of a *fair* volatility (at significance level α) may be understood as the volatility

$$\sigma(\alpha) := \text{sd}\left\{\ln\left(\frac{S(t)}{S(t-1)}\right) : \hat{H}_{t+1}^{2,\delta,n} \in \left[\frac{1}{2} \mp z_{1-\alpha/2}\sqrt{\text{Var}(\hat{H}_t^{2,\delta,n}|_{H(t)=1/2})}\right]\right\}.$$

where as usual $z_{1-\alpha/2} = \Phi^{-1}(1-\alpha/2)$ is the inverse cumulative distribution function (quantile function) of the standard normal distribution.

Data in Table 4 show the percentage of time the estimated Hurst exponent and the estimated volatility fall within the respective 95% efficient confidence interval. A comprehensive examination of how these metrics might be employed to assess degrees of market efficiency remains a valuable avenue for future research. The present study, therefore, focuses on providing the foundational data, leaving its detailed interpretation for subsequent analysis.

Table 4: Market Efficiency Metrics by Index. Percentage of time the estimated Hurst exponent and volatility are within the corresponding 95% efficient confidence interval.

Metric / Index		SPX	CCMP	SX5E	UKX	HSI	KLCI	KOSPI
Percentage	$\hat{H}_t^{2,\delta,n} \in$ 95%-CI	43.62	32.36	36.14	56.01	37.08	23.74	44.10
Percentage	$\hat{\sigma}(t) \in$ 95%-CI	50.65	46.37	41.02	53.31	59.52	28.15	45.35

		IMOEX	NIFTY	NKY	SET	SHCOMP	FSSTI	TWSE
Percentage	$\hat{H}_t^{2,\delta,n} \in$ 95%-CI	61.17	51.51	46.75	51.85	33.07	39.09	46.00
Percentage	$\hat{\sigma}(t) \in$ 95%-CI	14.23	27.56	47.43	56.21	50.72	41.74	45.21

The middle panels of Figures 3–16 offer empirical evidence that Proposition 1 holds. In all cases examined, the theoretical volatility determined using formula (8) is comparable to that estimated empirically, with the exceptions represented by outliers, where theoretical volatility is systematically higher than actual volatility. In addition to suggesting that the MPRE is definitely a good model for price dynamics in financial markets, the theoretical relationship identified allows us to respond to the primary requirement of this work, namely to link volatility to the time-varying dependence observed in the paths followed by prices (or indices in this case). The empirical validation of equation (8) establishes a foundation for deriving a fair volatility benchmark for any financial time series. Consequently, this framework provides a rigorous, model-based methodology to address a long-standing practical challenge: determining whether observed volatility is anomalously high or low at any point in time. This approach moves beyond traditional reliance on practitioner heuristics, ex-post portfolio analysis, or comparative measures like implied volatility. Instead, it enables a theoretically grounded assessment by quantifying the divergence between realized volatility and its efficient-market benchmark—the level expected if $H(t)$ were precisely $1/2$. This benchmark represents an equilibrium state toward which market prices gravitate to correct transient inefficiencies. The direction and magnitude of deviation from this equilibrium are economically informative. Significantly elevated volatility signals market roughness and negative autocorrelation—a state of heightened irregularity that typically triggers rapid mean-reversion. Conversely, suppressed volatility indicates excessive smoothness and positive autocorrelation, a condition of persistent regularity that often endures over longer

horizons. This asymmetry in market correction mechanisms finds a compelling explanation in the principles of behavioral finance. The cognitive and emotional biases detailed in Table 1—such as overreaction, herding, and loss aversion—provide a microstructure rationale for why markets correct disruptive volatility spikes more swiftly than they resolve periods of trending, but calmer, inefficiency.

5. Conclusion

This work establishes the Hurst-Hölder exponent as a superior, informationally equivalent substitute for volatility in financial risk measurement, provided price dynamics are locally fractional. Its adoption offers three principal advantages:

- *Path-Dependent Risk.* It directly quantifies path roughness, capturing deviations from semi-martingale behavior that volatility alone cannot. It moves beyond measuring mere variability to diagnosing the type and intensity of randomness.

- *Absolute Benchmarking.* Its value is intrinsically meaningful. Unlike volatility, which requires relative comparison, the exponent provides an absolute scale anchored by the martingale benchmark of $H(t) = \frac{1}{2}$.

- *Theoretical Synthesis.* It provides a contribution to resolve the apparent dichotomy between market efficiency and behavioral finance. These are not opposing models but alternating market phases, dynamically captured by the exponent's fluctuation around its efficient equilibrium.

The convertibility of Hurst-Hölder exponent into realized volatility is established by Proposition 1. This enables the determination of a confidence interval around the volatility level that prevails under conditions of informational market efficiency, that is, when prices exhibit submartingale behavior. This benchmark is the level that we termed *fair volatility*.

Consequently, volatility derived from the Hurst-Hölder exponent possesses a distinct advantage: it ceases to be a purely relative risk measure, assessable only in comparison to its own historical values; instead, it functions as an indicator of the market's deviation from its theoretical equilibrium.

Given the established mean-reverting property of the Hurst-Hölder exponent, the volatility calculated through the methodology described in this work is also informative of the subsequent correction required for the market to revert to equilibrium following a deviation. Further and more precise studies on the characteristics of the mean-reversion dynamics of the Hurst-Hölder exponent could provide the necessary framework for estimating the time required for this return to equilibrium.

Annex 1

Proof of Proposition 1.

We assume throughout:

H1 W is a standard Brownian motion independent of (H, ν).

H2 H and ν are almost surely continuous at t and take values in a compact subset $(\underline{H}, \overline{H}) \subset (0, 1)$ and $[\underline{\nu}, \overline{\nu}] \subset (0, \infty)$.

H3 $\int_{-\infty}^{t} \nu^2(s) \big[(t-s)_+^{H(s)-\frac{1}{2}} - (-s)_+^{H(s)-\frac{1}{2}} \big]^2 ds < \infty$ a.s. (this holds under **H1**–**H2**).

To simplify notation we write $H_t := H(t)$ and $\nu_t := \nu(t)$, and we prove the result for $h > 0$; the case $h < 0$ then follows by symmetry, yielding the factor $|h|^{H_t}$. We split the proof into the six following steps.

Step 1: Increment decomposition. For $h > 0$,

$$X_{t+h} - X_t = \int_{-\infty}^{t+h} \nu_s \Big[(t+h-s)_+^{H_s-\frac{1}{2}} - (-s)_+^{H_s-\frac{1}{2}} \Big] dW_s - \int_{-\infty}^{t} \nu_s \Big[(t-s)_+^{H_s-\frac{1}{2}} - (-s)_+^{H_s-\frac{1}{2}} \Big] dW_s$$

$$= \int_{-\infty}^{t} \nu_s \Big[(t+h-s)^{H_s-\frac{1}{2}} - (t-s)^{H_s-\frac{1}{2}} \Big] dW_s + \int_{t}^{t+h} \nu_s (t+h-s)^{H_s-\frac{1}{2}} dW_s,$$

since the $(-s)_+^{H_s-\frac{1}{2}}$ terms cancel for $s < 0$, and are zero for $s > 0$.

Step 2: Conditional Itô isometry. By **H1**, conditioning on $\mathcal{F}_t^{H,\nu}$ makes the integrands deterministic while preserving the Gaussianity/zero mean of the Itô integrals. Hence,

$$\mathrm{Var}\Big(X_{t+h} - X_t \,\big|\, \mathcal{F}_t^{H,\nu} \Big) = \int_{-\infty}^{t} \nu_s^2 \Big[(t+h-s)^{H_s-\frac{1}{2}} - (t-s)^{H_s-\frac{1}{2}} \Big]^2 ds + \int_{t}^{t+h} \nu_s^2 (t+h-s)^{2H_s-1} ds. \tag{10}$$

Step 3: Scaling change of variables. Set, for $s \leq t$, $u = (t-s)/h \in (0, \infty)$, i.e. $s = t - hu$, $ds = -h\, du$; and, for $s \in (t, t+h]$, $v = (t+h-s)/h \in (0, 1)$, $ds = -h\, dv$. Then (10) becomes

$$\mathrm{Var}\Big(X_{t+h} - X_t \,\big|\, \mathcal{F}_t^{H,\nu} \Big) = h^{2H_t} \bigg[\int_0^\infty \nu_{t-hu}^2\, h^{2(H_{t-hu}-H_t)} \Big[(u+1)^{H_{t-hu}-\frac{1}{2}} - u^{H_{t-hu}-\frac{1}{2}} \Big]^2 du$$

$$+ \int_0^1 \nu_{t+h(1-v)}^2\, h^{2(H_{t+h(1-v)}-H_t)}\, v^{2H_{t+h(1-v)}-1}\, dv \bigg]. \tag{11}$$

Step 4: Local freezing (continuity) and dominated convergence. By **H2**, as $h \downarrow 0$ we have

$$\nu_{t-hu} \to \nu_t, \qquad H_{t-hu} \to H_t \qquad \text{and} \qquad \nu_{t-h(1-v)} \to \nu_t, \ H_{t-h(1-v)} \to H_t,$$

uniformly over u in compact subsets of $(0, \infty)$ and v in $[0, 1]$.

Moreover, for all sufficiently small h,

$$\underline{H} < H_{t-hu}, H_{t-h(1-v)} < \overline{H}, \qquad \underline{\nu} \le \nu_{t-hu}, \nu_{t-h(1-v)} \le \overline{\nu}.$$

Hence the two integrands in (11) are dominated respectively by

$$C\left[(u+1)^{\overline{H}-\frac{1}{2}} - u^{\underline{H}-\frac{1}{2}}\right]^2 \quad \text{and} \quad C\, v^{2\underline{H}-1},$$

for a constant $C > 0$ independent on h; both are integrable on $(0, \infty)$ and $(0, 1)$ because, as $u \to \infty$, the difference behaves like $u^{\overline{H}-\frac{3}{2}}$ and thus its square is $u^{2\overline{H}-3}$ (integrable since $\overline{H} < 1$), while as $u \downarrow 0$ the term $u^{\underline{H}-\frac{1}{2}}$ yields square $u^{2\underline{H}-1}$ (integrable as $\underline{H} > 0$), and $v^{2\underline{H}-1}$ is integrable on $(0, 1)$.

Therefore we may pass to the limit $h \downarrow 0$ inside the brackets in (11) by dominated convergence, obtaining

$$\mathrm{Var}\left(X_{t+h} - X_t \,\middle|\, \mathcal{F}_t^{H,\nu}\right) = h^{2H_t}\nu_t^2\left[\underbrace{\int_0^\infty \left((u+1)^{H_t-\frac{1}{2}} - u^{H_t-\frac{1}{2}}\right)^2 du}_{=:J(H_t)} + \underbrace{\int_0^1 v^{2H_t-1}dv}_{=\frac{1}{2H_t}}\right] + o\left(h^{2H_t}\right)$$

$$= h^{2H_t}\nu_t^2\left(J(H_t) + \tfrac{1}{2H_t}\right) + o\left(h^{2H_t}\right). \tag{12}$$

Thus it remains to compute the constant

$$J(H) := \int_0^\infty \left((u+1)^{H-\frac{1}{2}} - u^{H-\frac{1}{2}}\right)^2 du \qquad (H \in (0, 1)).$$

Step 5: Evaluation of $J(H)$. Notice that $J(H)$ corresponds to the contribution from $s \le t$; the second integral in (12) supplies the contribution from $s \in (t, t+h]$. A direct way to evaluate $J(H)$ is via the Fourier transform of the kernel

$$k_H(u) := u_+^{H-\frac{1}{2}}, \qquad u \in \mathbb{R},$$

whose (tempered–distribution) Fourier transform is the classical formula (for $0 < H < 1$)

$$\widehat{k_H}(\omega) = \int_0^\infty u^{H-\frac{1}{2}}e^{-i\omega u}\, du = e^{-i\,\mathrm{sgn}(\omega)\,\frac{\pi}{2}\left(H+\frac{1}{2}\right)}\Gamma\left(H + \tfrac{1}{2}\right)|\omega|^{-H-\frac{1}{2}}.$$

Let $D_h k_H(u) := k_H(u + h) - k_H(u)$. By Parseval–Plancherel identity,

$$\int_\mathbb{R} \left(D_h k_H(u)\right)^2 du = \frac{1}{2\pi}\int_\mathbb{R} \left|(e^{i\omega h} - 1)\,\widehat{k_H}(\omega)\right|^2 d\omega = \frac{\Gamma\left(H+\frac{1}{2}\right)^2}{2\pi}\int_\mathbb{R} |e^{i\omega h} - 1|^2\, |\omega|^{-2H-1}\, d\omega.$$

Since $|e^{i\omega h} - 1|^2 = 2(1 - \cos(\omega h))$ and the integrand is even,

$$\int_\mathbb{R} \left(D_h k_H(u)\right)^2 du = \frac{2\Gamma\left(H+\frac{1}{2}\right)^2}{\pi}\int_0^\infty (1 - \cos(\omega h))\,\omega^{-2H-1}\, d\omega$$

$$= \frac{2\Gamma\left(H+\frac{1}{2}\right)^2}{\pi}\, h^{2H} \underbrace{\int_0^\infty (1 - \cos x)\, x^{-2H-1}\, dx}_{=:I(H)}. \tag{13}$$

21

Lemma (cosine integral). For $H \in (0, 1)$,

$$I(H) := \int_0^\infty (1 - \cos x)\, x^{-2H-1}\, dx = \frac{\pi}{2\,\Gamma(2H+1)\,\sin(\pi H)}.$$

Proof. Consider the classical identity (valid for $0 < \alpha < 2$)

$$\int_0^\infty (1 - \cos x)\, x^{-1-\alpha}\, dx = -\Gamma(-\alpha)\,\cos\left(\frac{\pi\alpha}{2}\right),$$

which follows by analytic continuation from $\int_0^\infty x^{\beta-1}\cos x\, dx = \Gamma(\beta)\cos(\pi\beta/2)$ for $\beta \in (0, 1)$. Setting $\alpha = 2H$ yields

$$I(H) = -\Gamma(-2H)\,\cos(\pi H).$$

Using $\Gamma(2H+1) = 2H\,\Gamma(2H)$ and the reflection identity $\Gamma(-2H)\Gamma(2H+1) = -\pi/\sin(2\pi H)$, we get

$$-\Gamma(-2H)\,\cos(\pi H) = \frac{\pi}{\Gamma(2H+1)} \cdot \frac{\cos(\pi H)}{\sin(2\pi H)} = \frac{\pi}{2\,\Gamma(2H+1)\,\sin(\pi H)}.$$

Substituting $I(H)$ into (13) gives

$$\int_{\mathbb{R}} \left(D_h k_H(u)\right)^2 du = \frac{2\Gamma\left(H+\frac{1}{2}\right)^2}{\pi}\, h^{2H} \cdot \frac{\pi}{2\,\Gamma(2H+1)\,\sin(\pi H)} = \frac{\Gamma\left(H+\frac{1}{2}\right)^2}{\Gamma(2H+1)\,\sin(\pi H)}\, h^{2H}.$$

On the other hand, a direct decomposition of the left–hand side over the regions $u > 0$, $-1 < u \leq 0$, $u \leq -1$ yields

$$\int_{\mathbb{R}} \left(D_h k_H(u)\right)^2 du = h^{2H}\left(\int_0^\infty \left((u+1)^{H-\frac{1}{2}} - u^{H-\frac{1}{2}}\right)^2 du + \int_0^1 v^{2H-1}\, dv\right) = h^{2H}\left(J(H) + \frac{1}{2H}\right).$$

Equating the two expressions and using $\Gamma(2H+1) = 2H\,\Gamma(2H)$ we obtain

$$J(H) + \frac{1}{2H} = \frac{\Gamma\left(H+\frac{1}{2}\right)^2}{\Gamma(2H+1)\,\sin(\pi H)} = \frac{\Gamma\left(H+\frac{1}{2}\right)^2}{2H\,\sin(\pi H)\,\Gamma(2H)} =: A(H).$$

This is the desired constant.

Step 6: Conclusion (variance and standard deviation). Combining (12) with the evaluation of $J(H)$ we have, as $h \downarrow 0$,

$$\mathrm{Var}\left(X_{t+h} - X_t \,\middle|\, \mathcal{F}_t^{H,\nu}\right) = h^{2H_t}\, \nu_t^2\, A(H_t) + o\left(h^{2H_t}\right).$$

Taking square roots (and using that $A(H_t) > 0$ and $h^{2H_t} \to 0$ so that the ratio of the square roots equals the square root of the ratio), we conclude

$$\mathrm{sd}\left(X_{t+h} - X_t \,\middle|\, \mathcal{F}_t^{H,\nu}\right) \sim |h|^{H(t)}\, \nu_t\, \sqrt{A(H(t))}, \qquad h \to 0,$$

which proves the claim.

$$\square$$

References

[1] D. Angelini and S. Bianchi. Nonlinear biases in the roughness of a Fractional Stochastic Regularity Model. *Chaos, Solitons & Fractals*, 172:113550, 2023.

[2] V.V. Anh, J.M. Angulo, and M.D. Ruiz-Medina. Possible long-range dependence in fractional random fields. *J. Statist. Planning & Inference*, 80:95–110, 1999.

[3] A. Ayache, C. Esser, and J. Hamonier. A new multifractional process with random exponent. *Risk and Decision Analysis*, 7(1-2):5–29, 2018.

[4] A. Ayache, S. Jaffard, and M. Taqqu. Wavelet construction of Generalized Multifractional processes. *Rev. Mat. Iberoamericana*, 23(1)(1):327–370, 2007.

[5] A. Ayache and J. Lévy Véhel. The Generalized Multifractional Brownian Motion. *Statistical Inference for Stochastic Processes*, 3(1-2):7–18, 2000.

[6] A. Ayache and M.S. Taqqu. Multifractional processes with random exponent. *Publicacionés Matemátiques*, 49:459–486, 2005.

[7] A. Benassi, P. Bertrand, S. Cohen, and J. Istas. Identification of the Hurst Index of a Step Fractional Brownian Motion. *Statistical Inference for Stochastic Processes*, 3(1-2):101–111, 2000.

[8] A. Benassi, S. Jaffard, and D. Roux. Gaussian processes and pseudodifferential elliptic operators. *Revista Mathematica Iberoamericana*, 13:19–89, 1997.

[9] S. Bianchi. Pathwise Identification of the memory function of the Multifractional Brownian Motion with Application to Finance. *International Journal of Theoretical and Applied Finance*, 8(2):255–281, 2005.

[10] S. Bianchi, D. Angelini, M. Frezza, and A. Pianese. From Fair Price to Fair Volatility: Towards an Efficiency-Consistent Definition of Financial Risk. *Preprint available at SSRN: https://ssrn.com/abstract=5395796 or http://dx.doi.org/10.2139/ssrn.5395796*, pages 1–32, 2025.

[11] S. Bianchi and A. Pantanella. Pointwise regularity exponents and well-behaved residuals in stock markets. *Int. J. of Trade, Economics and Finance*, 2(1):52–60, 2011.

[12] S. Bianchi, A. Pantanella, and A. Pianese. A dynamical assessment of stock market (in)efficiency, 2013.

[13] S. Bianchi, A. Pantanella, and A. Pianese. Modeling stock prices by multifractional Brownian motion: an improved estimation of the pointwise regularity. *Quantitative Finance*, 13(8):1317–1330, 2013.

[14] S. Bianchi, A. Pantanella, and A. Pianese. Efficient Markets and Behavioral Finance: a comprehensive multifractional model. *Advances in Complex Systems*, 18(1-2):1550001:1–1550001:29, 2015.

[15] S. Bianchi and A. Pianese. Time-varying Hurst–Hölder exponents and the dynamics of (in)efficiency in stock markets. *Chaos, Solitons & Fractals*, 109:64–75, 2018.

[16] Sergio Bianchi, Daniele Angelini, Augusto Pianese, and Massimiliano Frezza. Rough volatility via the lamperti transform. *Communications in Nonlinear Science and Numerical Simulation*, 127:107582, 2023.

[17] D.O. Cajueiro and B.M. Tabak. The Hurst exponent over time: testing the assertion that emerging markets are becoming more efficient. *Physica A: Statistical Mechanics and its Applications*, 336(3-4):521–537, 2004.

[18] P. Cheridito. Mixed Fractional Brownian Motion. *Bernoulli*, 7(6):913–934, 2001.

[19] J. F. Coeurjolly. Estimating the parameters of a fractional Brownian motion by discrete variations of its Sample Paths. *Statistical Inference for Stochastic Processes*, 4(2):199 – 227, 2001.

[20] J. F. Coeurjolly. Identification of multifractional Brownian motion. *Bernoulli*, 11(6):987 – 1008, 2005.

[21] F. Comte and E. Renault. Long memory in continuous-time stochastic volatility models. *Mathematical Finance*, 8(4):291–323, 1998.

[22] W.F.M. De Bondt and R. Thaler. Does the stock market overreact? *The Journal of Finance*, 40(3):793–805, 1985.

[23] L. Decreusefond and A. S. Üstünel. Stochastic analysis of the Fractional Brownian Motion. *Potential Analysis*, 10(2)(2):177–214, 1999.

[24] Iddo Eliazar. Power brownian motion. *Journal of Physics A: Mathematical and Theoretical*, 57(3):03LT01, dec 2023.

[25] Iddo I. Eliazar and Michael F. Shlesinger. Fractional motions. *Physics Reports*, 527(2):101–129, 2013. Fractional Motions.

[26] E.F. Fama. Efficient capital markets: A review of theory and empirical work. *The Journal of Finance*, 25(2):383–417, 1970.

[27] M. Frezza, S. Bianchi, and A. Pianese. Nonlinearity of the volume–volatility correlation filtered through the pointwise Hurst–Hölder regularity. *Communications in Nonlinear Science and Numerical Simulation*, 121:107204, 2023.

[28] M. Garcin. Forecasting with fractional Brownian motion: a financial perspective. *Quantitative Finance*, 22(8):1495 – 1512, 2022.

[29] J. Gatheral, T. Jaisson, and M. Rosenbaum. Volatility is rough. *Quantitative finance*, 18(6):933–949, 2018.

[30] C. Houdré and J. Villa. An example of infinite dimensional quasi-helix. *Contemporary Mathematics, Amer. Math. Soc.*, 336:195–201, 2003.

[31] J. Istas and G. Lang. Variations quadratiques et estimation de l'exposant de Hölder local d'un processus gaussien. *Ann. Inst. Henri Poincaré*, 33(4):407–436, 1997.

[32] J. T. Kent and A. T. A. Wood. Estimating the fractal dimension of a locally selfsimilar Gaussian process using increments. *J. of the Royal Stat. Soc. B*, 59(3):679–700, 1997.

[33] A. N. Kolmogorov. Wienersche spiralen und einige andere interessante kurven im hilbertschen raum. *C. R. (Doklady) Acad. Sci. URSS (N.S.)*, 26:115–118, 1940.

[34] M. Li. Multi-fractional generalized Cauchy process and its application to teletraffic. *Physica A: Statistical Mechanics and its Applications*, 550:123982, 2020.

[35] S.C. Lim and C.H. Eab. Some fractional and multifractional gaussian processes: A brief introduction. *Int. J. of Modern Physics: Conference Series*, 36:1560001, 2015.

[36] D. Loboda, F. Mies, and A. Steland. Regularity of multifractional moving average processes with random Hurst exponent. *Stochastic Processes and their Applications*, 140:21–48, 2021.

[37] P. Lévy. Sur certains processus stochastiques homogènes. *Compositio Mathematica*, 7:283–339, 1939.

[38] B.B. Mandelbrot and J.W. Van Ness. Fractional Brownian Motions, Fractional Noises and Applications. *SIAM Review*, 10(4):422–437, 1968.

[39] R. Mattera, F. Di Sciorio, and J.E. Trinidad-Segovia. A composite index for measuring stock market inefficiency. *Complexity*, Special Issue: Complexity Arising in Financial Modelling and its Applications:9838850 (13 pages), 2022.

[40] Sánchez-Granero M.J., M. Fernández-Martínez, and J.E. Trinidad-Segovia. Introducing fractal dimension algorithms to calculate the hurst exponent of financial time series. *The European Physical Journal B*, 85(86):1–13, 2012.

[41] R.S. Péltier and J. Lévy Véhel. Multifractional Brownian Motion: Definition and preliminary results. *Rapport de recherche INRIA 2645, Programme 4 (Robotique, Image et Vision - Action Fractales), 1-39*, pages 1–39, 1995.

[42] Q. Peng and R. Zhao. A general class of multifractional processes and stock price informativeness. *Chaos, Solitons & Fractals*, 115:248–267, 2018.

[43] A. Pianese, S. Bianchi, and A.M. Palazzo. Fast and unbiased estimator of the time-dependent Hurst exponent. *Chaos*, 28(31102):1–6, 2018.

[44] I.S. Reed, P.C. Lee, and T.K. Truong. Spectral Representation of Fractional Brownian Motion in n Dimensions and its Properties. *IEEE Transactions on Information Theory*, 41(5):1439–1451, 1995.

[45] M.A. Sánchez-Granero, K.A. Balladares, J.P. Ramos-Requena, and J.E. Trinidad-Segovia. Testing the efficient market hypothesis in latin american stock markets. *Physica A: Statistical Mechanics and its Applications*, 540:123082, 2020.